Investigation of the Phase Morphology of Dynamically Vulcanized PVC/NBR Blends Using Atomic Force Microscopy

S. M. Gheno,[1] F. R. Passador,[1] L. A. Pessan[2]

[1]*PPGCEM, Federal University of Sao Carlos, Sao Carlos 13565-905, SP, Brazil*
[2]*Department of Materials Engineering, Federal University of Sao Carlos, Sao Carlos 13565-905, SP, Brazil*

Received 26 May 2009; accepted 31 January 2010
DOI 10.1002/app.32195
Published online 3 May 2010 in Wiley InterScience (www.interscience.wiley.com).

ABSTRACT: Dynamic vulcanization is a mixing process employed in the melt state of elastomers with thermoplastics. This process may result in the formation of thermoplastic vulcanized (TPV) materials with improved properties such as mechanical strength, Young's modulus, hardness, and abrasion fatigue. In this study, a vulcanized thermoplastic was obtained by the dynamic vulcanization of poly(vinyl chloride)/acrylonitrile butadiene rubber (PVC/NBR) blends using a curative system based on sulfur (S)/tetramethylthiuram disulfide (TMTD) and mercaptobenzothiazyl disulfide (MBTS). The formation of crosslinks was characterized by differential scanning calorimetry (DSC) and Fourier transform infrared (FTIR) spectroscopy. The mechanical properties were analyzed by tensile tests and the phase morphology was investigated using atomic force microscopy (AFM) operating in the tapping mode-AFM. The phase images of the dynamically vulcanized blends showed an elongated morphology, which can be associated to the formation of crosslinks that give the material its excellent mechanical properties. © 2010 Wiley Periodicals, Inc. J Appl Polym Sci 117: 3211–3219, 2010

Key words: blends; dynamic vulcanization; atomic force microscopy

INTRODUCTION

Polymer blends have been employed to find new miscible combinations, since miscibility is a crucial factor in the development of the morphology of polymer blends.[1,2] To optimize processing and properties, it is important to know the polymer's melt rheology and the morphology of the resulting blend.[1–3]

PVC/NBR blends can be obtained as thermoplastic elastomers that look, feel and perform like vulcanized rubber.[4,5] As a broad generalization it may be said that in the blend the poly(vinyl chloride) (PVC) polymer contributes ozone, oil and fuel resistance, strength (tensile and tear), and stiffness, as well as weatherability, abrasion resistance, flame resistance, and higher electrical resistivity. Thus these properties of a nitrile rubber will be upgraded by modification with PVC.[6] Among the many different procedures to prepare PVC/NBR blends, the dynamic vulcanization of elastomer during its mixture in the molten state with a thermoplastic has been studied by many authors.[3–10] These systems have two main advantages over conventional systems, yielding vulcanized systems with reduced reversion and better aging characteristics.

The interaction parameter in PVC/NBR blends is very important because acrylonitrile-butadiene rubber (NBR) can act as a permanent plasticizer for PVC. Liu et al.[4–8] have presented extensive studies about PVC/NBR blends. These authors state that miscibility and interaction between phases, as well as dispersion of the rubber phase, are very important parameters for a better understanding of the performance of polymer blends. The pseudo-network morphology they obtained led to quantitative improvements in impact strength.

Dynamic vulcanization is a process whereby a thermoplastic and an elastomer are mixed in the melt state, with simultaneous crosslinking of the elastomer.[3,11,12] The quantity and type of crosslinking between the elastomeric chains formed during processing depend on the curative system used. Different curative systems give vulcanizates distinct properties with the same level of crosslinks, and the system to be chosen will depend on the anticipated use of the product.

The presence of double bonds in the butadiene unit of NBR normally facilitates its vulcanization with sulfur, but also makes it susceptible to oxidation and ozone attack. Accelerants reduce the time of vulcanization by increasing the speed of the

Correspondence to: S. M. Gheno (gheno@dema.ufscar.br).
Contract grant sponsor: CAPES.

reaction between sulfur and elastomer. Elastomer formulations may contain one or a combination of two types of accelerant.[4,7,13] Furthermore, Mousa et al.[14] studied dynamically cured PVC/NBR blends and found they exhibited improved oil resistance.

Tensile and impact properties are most commonly used to characterize the mechanical behavior of polymer blends. Some authors have reported that blend morphology is also very important in deciding about the ultimate properties of polymer blends.[15,16] In tensile measurements, stress–strain curves can reveal information about the deformation and the energy consumed before failure, in addition to ultimate strength and elongation properties.[17,18]

Many techniques have been used in the study of polymer blend surfaces and properties.[8,9,19–37] Among these techniques, atomic force microscopy (AFM) is an innovative tool that can map surface topography and phase heterogeneity simultaneously with high resolution up to the atomic level. Phase detection microscopy applied in experiments to investigate the mapping of different components is an important technique that has been used extensively in research, mainly in polymer science.[19–25]

Garcia et al.[26–33] stated that in dynamic AFM modes, tapping mode AFM (TM-AFM) is an important tool since it minimizes lateral forces. They demonstrated that phase shift measurements can be converted into energy dissipation values, and that energy dissipation maps provide an important method for the imaging of a material's properties because they do not depend directly on tip-surface interactions.

TM-AFM is an operational AFM mode which allows a second image—the phase image, also called phase contrast image—to be produced by using changes in the phase angle between the excitation and the oscillating tip of the AFM cantilever probe. Phase mapping takes place in response to the oscillation of the cantilever during the tapping mode scan. Phase imaging goes beyond simple topographical mapping to detect variations in composition, adhesion, viscoelasticity, and possibly other properties.[22,24,34]

Pickering and Vancso[35] studied polystyrene (PS) phase separates in cylinders contained within an amorphous polyisoprene (PI) matrix to determine the mole percentage of PS. Based on the fact that PS and PI have very different intrinsic properties, the authors used TM-AFM to study the contrast in the material's properties. The authors observed that the PS regions showed lower adhesion, which, in heterogeneous systems with components of different compliances and adhesion, could result in the observed changes and reversals in contrast images.

Magonov and Reneker[36] studied the application of state-of-the-art AFM methods to elucidate the surface and near-surface structure of polyethylene (PE) microlayers. The authors concluded that the stiffness-related contrast of the phase images offers new possibilities for imaging multicomponent polymer samples. This is confirmed by the phase images of several polymer systems.[36]

One of the purposes of this study was to produce dynamically vulcanized PVC/NBR blends and to investigate the influence of dynamic vulcanization on the mechanical properties and morphology, comparing them with the behavior of conventional noncrosslinked PVC/NBR blends, used in the automotive hose manufacture. Another goal was to develop the application and use of the tapping mode technique (TM-AFM) to obtain contrast formation in polymer phase imaging.

EXPERIMENTAL

Materials

The PVC used here was a suspension grade PVC resin (Norvic SP 1300HP, supplied by Braskem, Brazil) characterized by a K value of 71 ± 1. The plasticizer added to the system was an industrial grade dioctylphtalate (DOP) and the thermal stabilizer was an industrial grade barium and zinc base stabilizer. A commercial grade, partially crosslinked acrylonitrile-butadiene rubber (NBR) (Thoran NP-3351 C), containing 32.5 wt % of acrylonitrile supplied by Petroflex, Brazil, was used. Tetramethylthiuram disulfide (TMTD), mercaptobenzothiazyl disulfide (MBTS) and sulfur (S) were used as the accelerator-sulfur curative system, while a combination of zinc oxide (ZnO) and stearic acid was used as the activator system for the vulcanization of NBR.

Preparation of PVC and NBR compound

The compounding procedure was carried out as follows: The PVC was dry blended in an intensive mixer at 120°C with 60 parts per hundred of rubber (phr) of DOP and 3 phr of stabilizer, following the usual procedures. The NBR compound was also prepared in an intensive mixer at 90–100°C to prevent precuring during mixing. The formulation used in the preparation of the NBR compound was NBR = 100 phr, zinc oxide = 5 phr, stearic acid = 0.5 phr, TMTD = 1 phr, MBTS = 2 phr, and sulfur = 2 phr. First the NBR was mixed for 2 min, after which the other curing agents were added at 2-min intervals.

Preparation of blends

Two different types of PVC/NBR blends were prepared. The first system, called dynamically vulcanized blend (DB), was prepared using the PVC and NBR compound, while the second system, called

conventional blend (CB), was prepared with PVC and NBR compounds without the curing agents. The dynamically vulcanized PVC/NBR blends in ratios of 90/10, 80/20, and 70/30 wt % were produced by melt blending using a internal mixer (Haake, model Rheomix 600 rheometer) operating at 160°C with cam rotors running at 60 rpm for different mixing times. Samples were removed at 30-s intervals during mixing and immersed in liquid nitrogen to interrupt the reaction. The conventional blends of PVC/NBR (90/10, 80/20, and 70/30 wt %) were melt-mixed using the Haake Rheomix 600 at 160°C and a cam rotor speed of 60 rpm for 5 min. The blends used in this work were given the following acronyms: CB = conventional blend, DB = dynamically vulcanized blend, while the numbers indicate the weight percentage of NBR in the blend. NBR u and NBR c indicate NBR uncrosslinked and crosslinked, respectively.

Crosslink formation

Fourier transform infrared (FTIR) spectroscopy analyses were performed using a Nicolet 4700 spectrophotometer (Thermo Electron Corp.) on 2 mm thick samples on a KBr disc. The degree of cure was calculated using differential scanning calorimetry at different mixing times. The heat of reaction was measured with a QS 100 thermal analyzer (TA Instruments) at a heating rate of 20°C/min from room temperature to 300°C. The total amount of heat used in the thermal crosslinking reaction can be related to the exothermic peak areas of the DSC curves. The degrees of cure were calculated based on the residual heat from the thermal crosslinking of the crosslinked samples. The reference heat value for the completely crosslinked sample was considered as the heat of the thermal crosslinking of the uncrosslinked formulation. The degree of cure was calculated from eq. (1).

$$\text{Degree of cure}(\%) = \left[1 - \frac{\Delta H_{\text{residual cure}}}{\Delta \text{H}_{\text{total cure}}}\right] \times 100 \quad (1)$$

where $\Delta H_{\text{total cure}}$ corresponds to the value of residual heat from thermal crosslinking of partially cured samples, and $\Delta H_{\text{residual cure}}$ corresponds to the residual heat of the completely cured sample. The procedure used to determined $\Delta H_{\text{total cure}}$ and $\Delta H_{\text{residual cure}}$ was described by Ruiz.[37] The crosslink densities of the samples were measured by a swelling method, as follows. First the PVC was removed by Soxhlet extraction with acetone (C_3H_6O) for 20 h; then the samples were soaked in methyl ethyl ketone (MEK) for 22 h, the weight of the swollen samples was measured and the crosslink density calculated. The solubility parameter of MEK and NBR are 9.27 and 9.25 $(\text{cal/cm}^3)^{0.5}$, respectively. An χ (interaction parameter between the rubber network and the swelling agent) of 0.44, a bulk density of rubber of 1.01 g/cm^3, and a molar volume of MEK of 89.7 $\text{cm}^3\ \text{mol}^{-1}$ were employed.

Mechanical testing

For each compound under study, a sheet about 2.0 mm thick was prepared by compression molding at 160°C for 4 min, after which samples were cut into different geometries, according to the standard required for each analysis, using a pneumatic die cutter (Ceast). The main mechanical tests were carried out as follows: (i) "Tensile Tests" were carried out on a MTS Universal Testing Machine (Alliance RT/5) according to the ASTM D 638 standard. The cross-head speed was 500 mm/min. Five specimens were used and the median value was taken in each case. (ii) "Tear Tests" were carried out according to the ASTM D 1004 standard on a MTS Universal Testing Machine (model Alliance RT/5) at a cross-head speed of 51 mm/min. Five specimens were used and the average value was calculated.

AFM experiments

Samples of the blends were cryogenically cracked in liquid nitrogen to prevent possible phase deformation. Simultaneously, tapping mode topography and phase images were viewed side-by-side in real time at a scan speed of 0.8 Hz. In phase imaging, the phase lag of the cantilever oscillation, relative to the signal sent to the cantilever's piezodriver, is simultaneously monitored by the Quadrex Module and recorded by the Nanoscope IIIa SPM controller (Digital Instruments/Veeco Metrology, Santa Barbara, CA). The sample's free surface was imaged using an NSC15 (MikroMasch) tip, radius <10 nm. The average force constant was 45 N/m and a resonance frequency between 265 and 400 kHz was used for imaging in TM-AFM. Imaging was carried out at room temperature. Before the tip engaged the sample, the phase of the free cantilever oscillation was adjusted. The tip-to-sample force can be varied by changing the driving amplitude (Da) and the set-point amplitude (Asp). The tip-to-sample force parameters used in this study were: a typical free amplitude (Ao) of 2.0 V and a set-point amplitude of 2.0 V after tuning. The set-point amplitude can be altered from 1.0 to 1.8 V during scanning. The typical driving amplitude of the NSC15 tip was 50 mV. The same tip was used for imaging in all the TM-AFM analyses. Imaging was carried out at room temperature.

RESULTS AND DISCUSSION

Rheometric torque curves

Figure 1 shows the rheometric torque curves of vulcanized blends. The first peak corresponds to the addition of the compounds. The torque increased with increasing mixing time in response to the formation of crosslinks in the elastomeric phase. PVC/NBR blends with high NBR content showed vulcanization reaction in shorter mixing times due to the difference in viscosity between the PVC matrix and the elastomeric phase. The NBR had a higher viscosity than the PVC matrix. Therefore, the increase in elastomer content in the blend increased the friction between the PVC and NBR particles during mixing, causing the temperature of the material to rise and offering ideal conditions for NBR crosslinking. The values of maximum torque are usually proportional to the density crosslinks of formed by the volume of elastomer. In our system, the larger amount of accelerant than of sulfur generated an efficient system, whose main feature was the formation of mono- and polysulfides bound together in large quantities, as described in the literature.[13]

Crosslink formation

The formation of crosslinks was analyzed by FTIR and by measurements of the degree of cure during mixing of the blends. Figure 2 shows the infrared spectra of the PVC compound, crosslinked and uncrosslinked NBR, and the PVC/NBR blends. In Figure 2(a), the band at 1723 cm^{-1} is assigned to the C=O stretching vibration and corresponds to a small quantity of double bond structures of DOP, while the bands at about 1600, 1580, 1462 and 1435 cm^{-1} are assigned to the aromatic C=C stretching vibration and the band at about 743 cm^{-1} is assigned to the ortho di-substituted ring deformation, also characteristic of DOP. The bands at 1124 and 1073 cm^{-1} correspond to the C—C stretching vibration of PVC. The characteristic bands at 1274 cm^{-1} and 960 cm^{-1} are assigned to the CH_2—Cl stretching vibration and the C—Cl stretching vibration of PVC, respectively. The band at about 690 cm^{-1} corresponds to the C—H deformation of PVC.[38]

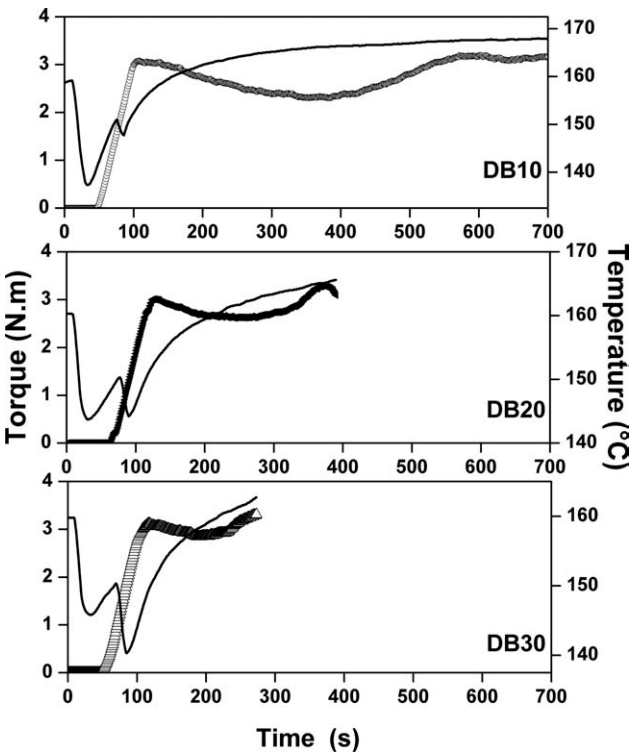

Figure 1 Variation of torque and temperature during mixing of dynamic vulcanized blends of PVC/NBR.

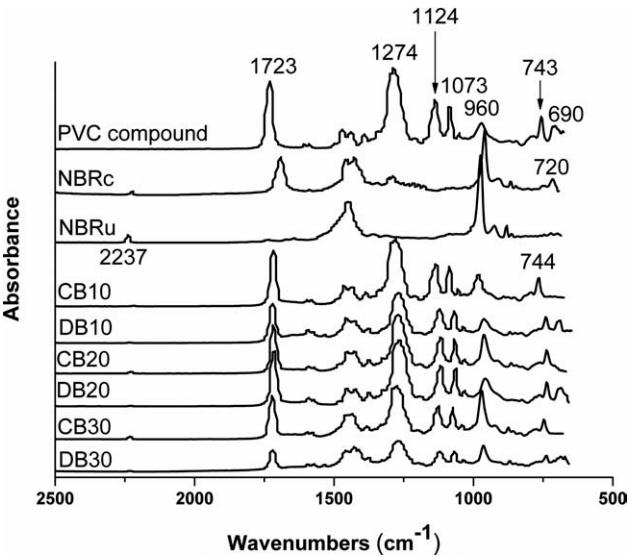

Figure 2 Infrared spectra of the compounds.

The chemical structure of NBR can be represented by three possible isomeric structures for the butadiene segments. The band at 2237 cm^{-1} is assigned to the —CN stretching vibration, which is characteristic of NBR. The characteristic band at 1720 cm^{-1} is assigned to the C=C deformation vibration of NBR. The bands at about 1465 cm^{-1} and 1450 cm^{-1} correspond to the CH_3 stretching vibration and C—H aliphatic vibration, respectively, while the band at 968 cm^{-1} is assigned to the cis-1,4-butadiene angular deformation, which is characteristic of NBR. The main difference between the crosslinked and uncrosslinked NBR is the band at 720 cm^{-1} assigned to the C—S stretching vibration, which was a result of crosslink formation.

The acrylonitrile-butadiene rubber was vulcanized using an activation system followed by the addition of sulfur. Sulfur vulcanization occurs through radical

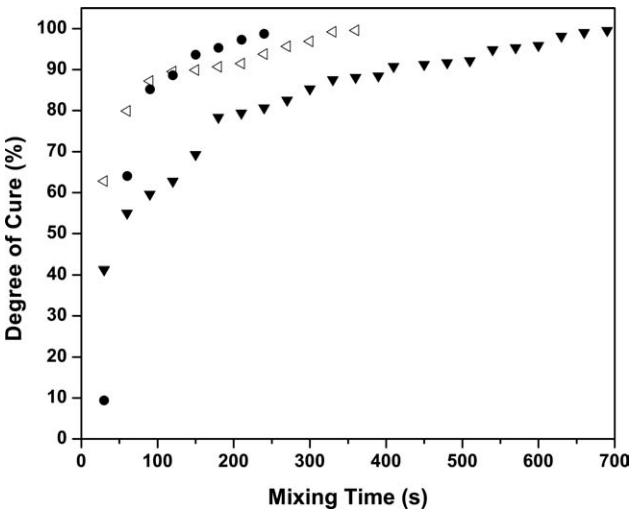

Figure 3 Degree of cure (%) versus mixing time (s): DB 10 (▼), DB 20 (◁) and DB 30 (●).

substitution in the form of polysulfide bridges and sulfur via intracyclization with the polymer molecules.

The bands observed in the infrared spectra of the blends correspond to the PVC phase and the NBR phases. In the dynamically vulcanized blends (DB), the presence of a band at 720 cm^{-1}, which is assigned to the C—S stretching vibration, resulted from crosslinking during the reactive process. This band was not observed in the conventional blends.

The degree of cure was measured based on eq. (1). The $\Delta H_{\text{total cure}}$ values of the blends were 2.18, 2.58, and 2.56 J g^{-1} for the dynamically vulcanized blends DB 10, DB 20, and DB 30, respectively. The samples collected at 30-second intervals during mixing were subjected to DSC analyses of $\Delta H_{\text{residual cure}}$. Figure 3 shows the degree of cure versus mixing time of the dynamically vulcanized blends.

Increasing the mixing time promoted dynamic vulcanization of the acrylonitrile-butadiene rubber in all the systems. Long mixing times increased the degree of cure because there was sufficient time for the formation of crosslinks. It has long been known that prolonging the processing time of rubber compounds can heighten the degree of vulcanization and simultaneously increase crosslinking. The effectiveness of the curing agent also depends on the temperature reached during the mixing process and, as the temperature rises in response to increasing friction, the increasing rubber content in the system increases the crosslinking reactions due to the higher temperature during mixing.

Further evidence of crosslinking in the systems was provided by the results of the swelling studies. The curative system used in this study was designed to promote crosslinking only of the NBR phase; thus, no reaction occurred between PVC and NBR. The extraction process in acetone allowed for the extraction of 85% of the PVC phase. Swelling studies were done in methyl ethyl ketone (MEK), which is able to dissolve and swell only the NBR phase. The crosslink density values obtained for NBRc, DB 10, DB 20, and DB 30 were 4.1×10^{-4} mol/cm^3, 1.2×10^{-4} mol/cm^3, 1.3×10^{-4} mol/cm^3 and 1.9×10^{-4} mol/cm^3, respectively. The results were normalized according to the amount of residual PVC in the blends. The PVC remaining after extraction can limit the swelling of NBR, decreasing the blends' crosslink densities. Increasing the rubber content in the dynamically vulcanized blends augmented the crosslink density. Thus, crosslinking in the blends was indicated by the increase in the degree of cure and the crosslink density values.

Mechanical properties

The mechanical strength of the PVC compound, NBR, conventional PVC/NBR blends, and dynamically vulcanized PVC/NBR blends with different NBR contents was evaluated by tensile and tear strength tests.

Tensile tests

Table I lists the results of the tensile tests, i.e., tensile strength (σ_r), elongation at break (ε_r) and Young's modulus (E).

The tensile test results indicated that the pure NBRu had a low tensile strain and that the vulcanization process (NBRc) augmented the tensile strain and mechanical strength of NBR.[4] The change in NBR content in the conventional blends led to an increase of tensile strain when compared with that of NBRu. Note that the tensile strain decreased as the NBRu content increased. All the dynamically vulcanized blends showed higher tensile strength values than those of the conventional blends. The vulcanization process stiffened the NBR phase,

TABLE I
Tensile Strength (σ_r), Elongation at Break (ε_r), and Young's Modulus (E) of PVC Compound, NBR, and PVC/NBR Blends

Sample	σ_r (MPa)	ε_r (%)	E (MPa)
PVC compound	15.2 ± 0.2	411.6 ± 11.6	10.5 ± 0.2
NBR u	0.4 ± 0.1	605.8 ± 24.3	1.4 ± 0.1
NBR c	3.1 ± 0.3	200.9 ± 9.5	2.1 ± 0.1
CB 10	10.7 ± 0.4	406.3 ± 1.7	6.9 ± 0.2
DB 10	13.3 ± 0.3	287.8 ± 9.1	7.7 ± 0.1
CB 20	7.6 ± 0.1	595.4 ± 11.8	1.6 ± 0.1
DB 20	13.8 ± 0.2	408.5 ± 6.1	5.1 ± 0.1
CB 30	7.7 ± 0.2	347.3 ± 4.9	4.5 ± 0.1
DB 30	14.8 ± 0.2	348.1 ± 6.1	6.3 ± 0.1

contributing to increase the mechanical strength of the blends.[13]

The formation of crosslinks reduces elongation at break due to the presence of reticulated rubber particles that act to diminish the elasticity of blends, thereby increasing the stiffness of the elastomeric phase. Thus, the dynamically vulcanized blends showed lower values of elongation at break due to the formation of reticulates in the elastomer lattices.

Reactive processing increases the stiffness of the elastomeric phase, so an increase in Young's modulus is expected. Increasing the NBR content in the conventional blends caused their Young modulus to decrease in comparison with that of the PVC compound and of the dynamically vulcanized blends. Crosslinking increased the Young modulus of the vulcanized blends because of the greater degree of reticulation, which in turn increased the stiffness of the elastomeric phase. The curative system based on the mixture of accelerants and sulfur improved the mechanical performance of the vulcanized blends when compared with that of the conventional blends. For example, DB10 showed an increase of 205% in the value of Young's modulus compared with that of CB10.

Tear tests

Figure 4 shows the results of tear strength tests of the PVC compound, acrylonitrile-butadiene rubber, conventional and vulcanized blends. The results indicate that the increase in NBR content reduced the tear strength of the blends. This reduced tear strength is due to the low cohesion between the elastomeric chains in uncrosslinked NBR. Thus, the tear fracture of the NBRu is governed by cohesive control.[39] The conventional blends showed low tear strength when compared to that of the PVC compound. Increasing the NBR content in the conventional blends reduced the values of tear strength due to low interactions in the uncrosslinked NBR, and consequently, low cohesive force. On the other hand, the vulcanization process increased the tear strength due to the formation of reticulates in the rubber chains. Furthermore, the crosslinking reactions that occur during reactive processing lead to the formation of rigid segments which are responsible for increasing the cohesion of elastomeric chains.[40] This fact was confirmed especially in the composition with higher NBRc content, which showed a 370% increase in DB30 compared with CB30. This finding is coherent with the fact that the greater tear strength of vulcanized blends is directly related to their crosslink density. The samples with high crosslink density showed an increase in tear strength; however, the size and distribution of the dispersed phases formed during processing must also be taken into account. All these factors are responsible for the mechanical performance of polymers blends.

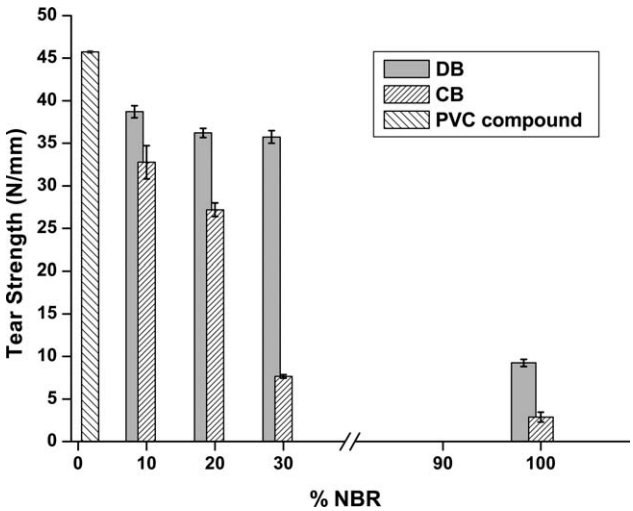

Figure 4 Tear strength of the samples.

Atomic force microscopy

AFM surface and phase imaging were used to characterize the conventional and vulcanized blends (Figs. 5 and 6). The images show dark and bright regions corresponding to the valleys and hills of the surface. The morphology depicted in these images is important to identify the phase-separated regions and understand the phase contrast between these regions. Phase imaging was performed simultaneously with tapping mode scan to detect variations in viscoelasticity and elasticity.

Figure 5 shows AFM images of the CB PVC/NBR series. The surface images of CB 10, CB 20, and CB 30 obtained in tapping mode are presented in Figure 5(a), (c), and (e), respectively. The phase images led to the identification and mapping of different components in CB PVC/NBR samples through differences in contrast. Figure 5(b), (d), and (f) show a two-phase structure of the polymer blend clearly defined by the high resolution of the phase imaging: the highlighted portions of the images show the NBR phase, while the dark contrast in the image corresponds to low elasticity, i.e., the PVC phase.

The morphology of CB PVC/NBR [Fig. 5 (b,d,f)] shows spherical elastomer particles dispersed in the PVC matrix. It was observed that increasing the NBR content in the blends augmented the particle size, possibly as a result of the particle coalescence phenomenon.

The shape and size of particles obtained by contrast in the phase images is governed by many factors that affect tip-sample interactions including the mechanical properties and elastic inhomogeneity.

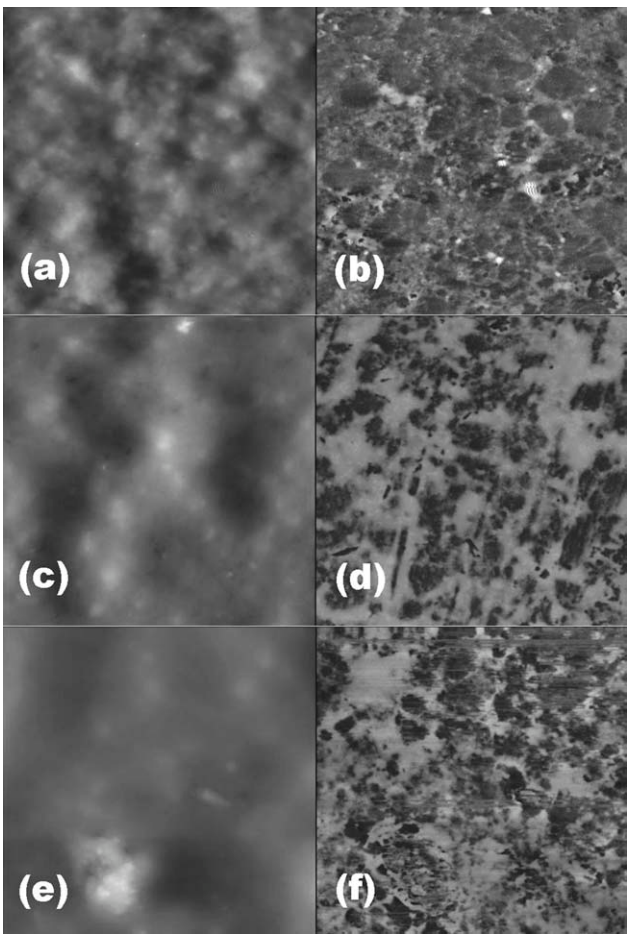

Figure 5 Tapping mode images of CB PVC/NBR (10 μm ×10 μm). CB 10: topographic (a) and phase shift (b); CB 20: topographic (c) and phase shift (d), and CB 30: topographic (e) and phase shift (f).

May be the higher friction can be responsible for the variation in particle size of the elastomeric phase and for the good dispersion of particles in the thermoplastic matrix.

Figure 6 shows AFM images of DB PVC/NBR series. Figure 6(a), (c), and (e) show the tapping mode images of DB 10, DB 20, and DB 30, respectively. The images show a two-phase structure of the polymer blend clearly defined by the high resolution of the phase imaging: the highlighted parts of the images represent the NBR phase, while the dark contrasts indicate low elasticity, i.e., the PVC phase.

The results presented in Figures 5 and 6 indicate that the elasticity of the conventional and vulcanized blends was higher than that of the PVC matrix in which they were embedded. The contrast obtained in the phase images is governed by many factors that affect tip-sample interactions, including the material's mechanical properties and elastic inhomogeneity. Phase imaging provided strong contrast, revealing both CB and DB in great detail in the PVC matrix. The size and shape of the phases varied with the CB and DB content in the sample.

The dynamic vulcanization process increased the stiffness of the elastomeric phase, leading to the differences in morphology of the two systems under study. The phase images of the dynamically vulcanized blends showed a morphology of well dispersed and elongated elastomeric particles in the PVC matrix. The formation of crosslinks during reactive processing reduced the particle size of the NBR phase due to the greater friction between the particles, causing the elastomeric particles to break up. Phase morphology with small particle sizes and a well dispersed elastomeric phase improves the mechanical properties. The increase of elastomeric phase in DB PVC/NBR blends has been attributed to the greater degree of cure and, hence, higher crosslink density.

The literature contains reports of several studies using the AFM technique, which can be used to

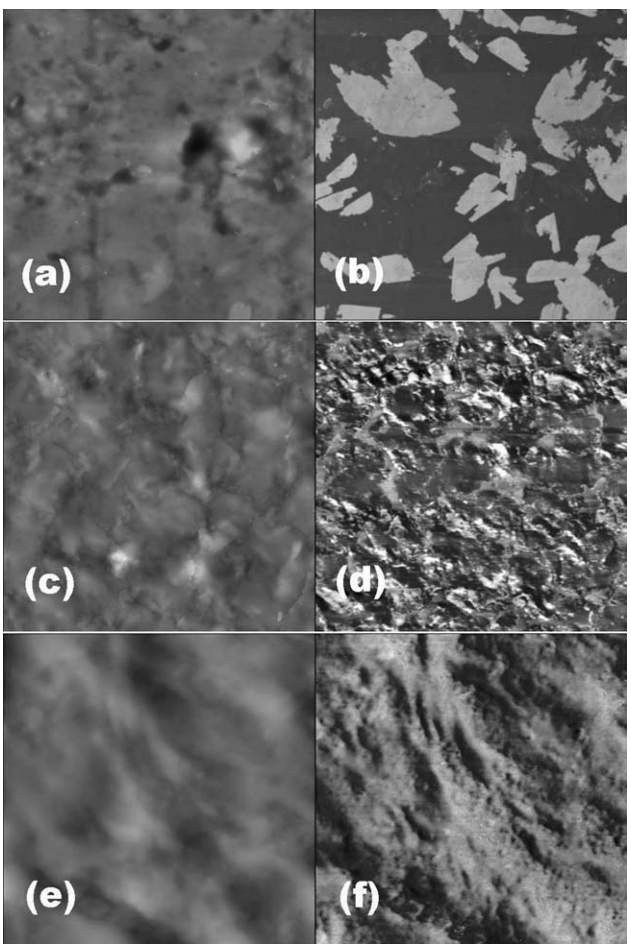

Figure 6 Tapping mode images of DB PVC/NBR (10 μm ×10 μm). DB 10: topographic (a) and phase shift (b); DB 20: topographic (c) and phase shift (d), and DB 30: topographic (e) and phase shift (f).

quantify the properties of polymer systems.[2,14,19,20,39,41–44] The phase images in Figures 5 and 6 provide the best contrast of morphological features due to the high sensitivity of the TM-AFM technique. The results obtained in this work are supported by studies conducted by Efimov et al.,[40] Magonov and Reneker,[36] Pickering and Vancso,[35] and Jang Liu.[45]

The mapping of different components by phase detection microscopy is a very useful technique that has been used extensively in research, especially in polymer science. The image analysis based on phase imaging yielded information on particle size and size distribution and has become an alternative analytical method to the traditional TEM characterization of materials with different phases and polymer blends.[46] A study reported by Jiang Liu[45] showed that in the presence of weak forces of interaction, the contrast is influenced by differences in adhesion force, as shown in Figures 5 and 6 for the PVC matrix, and the CB PVC/NBR and DB PVC/NBR samples. Phase images are related directly to the material's density and elastic modulus, and the stiffness-related contrast of the phase images offers new possibilities for imaging multicomponent polymer samples.[36]

CONCLUSIONS

Dynamically vulcanized PVC/NBR blends were obtained through reactive processing, using a curative system based on sulfur and a mixture of accelerants. The phenomenon of crosslinking is crucial in the improvement of these materials' mechanical properties. The dynamically vulcanized blends showed higher tensile strength and Young's modulus than the conventional blends. The vulcanization process increased the stiffness of the elastomeric phase, contributing to increase the mechanical strength of the blends. Curing also affected the tear strength values. The phase morphology of the blends, which was analyzed using a powerful tool for mapping variations in a sample's properties at very high resolution, was strongly affected by the processing system. Phase images revealed a two-phase structure in the polymer blend, which was clearly defined by the high resolution of the phase imaging, indicating that the elasticity of the conventional and vulcanized blends was greater than that of the PVC matrix in which they were embedded. Phase detection microscopy proved to be a very useful tool to obtain contrasts in polymer phase imaging.

The authors gratefully acknowledge Braskem S. A. for the donation of PVC, the NEO-PVC Program for its technical support.

References

1. Utracki, L. A.; Favis, B. D. In Handbook of Polymers Science and Technology, Cheremisinoff, N. P., Ed.; Hanser: Munich, 1989; p 125.
2. Corradini, E.; Rubira, A. F.; Muniz, E. C. Eur Polym J 1997, 33, 1651.
3. Passador, F. R.; Rodolfo, A., Jr.; Pessan, L. A. Pol: Ciênc Tecnol 2008, 18, 193.
4. Liu, Z. H.; Zhu, X.; Wu, L.; Li, R. Y.; Qi, Z.; Choy, C.; Wang, F. Polymer 2001, 42, 737.
5. Liu, Z. H.; Wu, L. X.; Kwok, K. W.; Zhu, X. G.; Qi, Z. N.; Choy, C. L.; Wan, F. S. Polymer 2001, 42, 1719.
6. Titow, W. V. PVC Technology, 4th ed.; Elsevier Applied Science pubication: New York, 1984.
7. Liu, Z. H.; Zhang, X. D.; Zhu, X. G.; Li, R. K. Y.; Qi, Z. N.; Wang, F. S.; Choy, C. L. Polymer 1998, 39, 5019.
8. Liu, Z. H.; Zhang, X. D.; Zhu, X. G.; Li, R. K. Y.; Qi, Z. N.; Wang, F. S.; Choy, C. L. Polymer 1998, 39, 5027.
9. Akiba, M.; Hashim, A. S. Prog Polym Sci 1997, 22, 475.
10. Coran, A. Y. In Handbook of Elastomers—New Developments and Technology, Stephens, H. L., Ed.; Dekker Inc: New York, 1988.
11. Hafezi, M.; Khorasani, S. N.; Ziaei, F.; Azim, H. R. J Elastom Plast 2007, 39, 151.
12. Jacobi, M. M.; Schneider, L. K.; Freitas, L. L.; Schuster, R. H. Raw Mat Appl 2006, 49.
13. Oliveira, M.; Soares, B. G. Pol: CiêncTecnol 2002, 12, 11.
14. Mousa, A.; Ishiaku, U. S.; Ishak, Z. A. M. Polym Bull 2005, 53, 203.
15. Kolarik, J.; Lednicky, F.; Locati, G.; Fambri, L. Polym Eng Sci 1997, 37, 128.
16. Bagheri, R.; Pearson, R. A. J Mat Sci 1996, 31, 3945.
17. Jones, M. A.; Carriere, C. J.; Dineen, M. T.; Balwinski, K. M. J ppl Polym Sci 1997, 64, 673.
18. Castellani, L.; Maestrini, C. Polymer 1990, 31, 2278.
19. Painter, P. C.; Graf, J. F.; Coleman, M. M. Macromolecules 1991, 24, 5630.
20. George, K. E.; Rani, J.; Francis, D. J. J Appl Polym Sci 1986, 32, 2867.
21. Passador, F. R.; Rodolfo, A, Jr.; Pessan, L. A. J Macromol Sci B: Phys 2009, 48, 282.
22. San Paulo, A.; García, R. Biophys J 2000, 78, 1599.
23. Magonov, S. N.; Elings, V.; Whangbo, M. H. Surf Sci 1997, 375, L385.
24. Raghavan, D.; Vanlandingham, M.; Gu, X.; Nguyen, T. Langmuir 2000, 16, 9448.
25. Raghavan, D.; Gu, X.; Nguyen, T.; Vanlandingham, M.; Karim, A. Macromolecules 2000, 33, 2573.
26. Garcia, R.; Calleja, M.; Pérez-Murano, F. Appl Phys Lett 1998, 72, 2295.
27. Garcia, R.; San Paulo, A. Ultramicroscopy 2000, 82, 79.
28. Tamayo, J.; Garcia, R. Langmuir 1996, 12, 4430.
29. Burham, N. A.; Behrend, O. P.; Ouveley, F.; Gremaud, G.; Gallo, P. J.; Gordon, D.; Dupas, E.; Kulik, A. J.; Pollock, H. M.; Briggs, G. A. D. Nanotech 1997, 8, 67.
30. Garcia, R.; San Paulo, A. Phys Rev B 1999, 60, 4961.
31. Garcia, R.; San Paulo, A. Phys Rev B 2000, 61, 13381.
32. Rodriguez, T. R.; Garcia, R. Appl Phys Lett 2002, 80, 1646.
33. Garcia, R.; Perez, R. Surf Sci Rep 2002, 47, 197.
34. Stark, M.; Möller, C.; Müller, D. J.; Guckenberger, R. Biophys J 2001, 80, 3009.
35. Pickering, J. P.; Vancso, G. J. Polym Bull 1998, 40, 549.
36. Magonov, S. N.; Reneker, D. H. Annu Rev Mat Sci 1997, 27, 175.
37. Ruiz, C. S. B.; Machado, L. D. B.; Pino, E. S.; Sampa, M. H. O. J Therm Anal Cal 2002, 63, 481.
38. Pielichowski, K. J Therm Anal Cal 1999, 55, 559.

39. Wang, Q.; Zhang, X.; Liu, S.; Gui, H.; Lai, J.; Liu, Y.; Gao, J.; Huang, F.; Song, Z.; Tan, B. H.; Qiao, J. Polymer 2005, 46, 10614.
40. Efimov, A. E.; Tonevitsky, A. G.; Dittrich, M.; Matsko, N. B. J Microsc 2007, 226, 207.
41. Almeida, C. L.; Akcelrud, L. C. Pol: Ciênc Tecnol 1999, 9, 23.
42. Ismail, H.; Tan, S.; Poh, B. T. J Elastom Plast 2001, 33, 251.
43. Shen, F.; Li, H.; Wu, C. F. J Polym Sci Part B: Polym Phys 2006, 44, 378.
44. Passador, F. R.; Rodolfo, A., Jr.; Pessan, L. A. Pol: Ciên Tecnol 2006, 16, 174.
45. Liu, J. Microsc Microanal 2003, 9, 452.
46. Passador, F. R.; Rodolfo, A., Jr.; Pessan, L. A. Pol: Ciênc Tecnol 2007, 17, 80.